Original Research

Subacute Sclerosing Panencephalitis: Relationship Between Clinical Stage and Diffusion-Weighted Imaging Findings

Alpay Alkan, MD,[1]* Levent Korkmaz, MD,[2] Ahmet Sigirci, MD,[1] Ramazan Kutlu, MD,[1] Cengiz Yakinci, MD,[2] Gulnur Erdem, MD,[1] and Saim Yologlu, PhD[3]

Purpose: To investigate the relationship between clinical stages and apparent diffusion coefficient (ADC) changes in the brain of patients with subacute sclerosing panencephalitis (SSPE).

Materials and Methods: A total of 18 patients with stage II (N = 11) and III (N = 7) SSPE and 11 age-matched controls underwent routine MRI and diffusion-weighted imaging (DWI). The ADC values were automatically calculated. Seven distinct neuroanatomic structures (frontal, parieto-occipital, and cerebellar white matter; deep white matter; thalamus; basal ganglia; and brainstem) were selected for analysis in the patient and control groups.

Results: Hyperintensities in the periventricular and subcortical white matters on T2-weighted images and ADC maps were detected in 63.6% of patients with stage II and in all patients with stage III. There were significant differences between stage II and III patients and also between patients and control group in ADC values that obtained from all locations. The highest mean ADC values were calculated in stage III patients. Although MRI and DWI findings were normal in four patients with stage II disease, ADC values were significantly increased when compared with controls.

Conclusion: The stage of disorder may be independent of DWI appearance during the early stage (stages I and II), even though the brain is affected. Therefore, DWI and ADC values supplemental to routine MRI should also be utilized for lesion detection and definition to enhance diagnostic accuracy in patients with SSPE.

Key Words: subacute sclerosing panencephalitis; MRI; diffusion-weighted imaging; apparent diffusion coefficient; stage
J. Magn. Reson. Imaging 2006;23:267–272.

SUBACUTE SCLEROSING PANENCEPHALITIS (SSPE) is a slow virus infection caused by the measles virus. It is a fatal, incurable, inflammatory, and neurodegenerative disease that causes death within 2–4 years of onset (1,2).

MRI findings are usually not correlated with the clinical stage of the disease. It is not possible to define these findings as improvement or progression based on the MRI findings alone (3–8). A few studies have evaluated diffusion-weighted imaging (DWI) and MR spectroscopy (MRS) findings in patients with SSPE (8–11). DWI and apparent diffusion coefficient (ADC) maps provide unique information about the viability of brain tissue. Even subtle pathological damage should disrupt the tissue architecture and increase the mobility of water molecules, thereby giving ADC maps the potential to detect structural changes that are inaccessible to conventional MRI (12). Diffusion of water is restricted because of cytotoxic edema, and ADC values decline. Regions of vasogenic edema demonstrate increased ADC as a result of the diffusion of water in the extracellular compartment (13,14).

Periventricular and subcortical hyperintensities on T2-weighted imaging in patients with SSPE have been reported in the literature (2,15,16). These lesions may reveal vasogenic edema-like increased diffusion and ADC values that are more likely related to major neuronal impairment or loss (10,11). Oksuzler et al (11) reported that increased ADC values were obtained from normal-appearing white matter (NAWM) on MRI and DWI in a patient with SSPE. They stressed the need for further studies to evaluate DWI and ADC values in NAWM (11).

The purpose of this study was to investigate the relationship between clinical stages and ADC changes in the brain of patients with SSPE.

[1]Department of Radiology, Inonu University School of Medicine, Malatya, Turkey.
[2]Department of Pediatrics, Inonu University School of Medicine, Malatya, Turkey.
[3]Department of Biostatistics, Inonu University School of Medicine, Malatya, Turkey.
*Address reprint requests to: A.A., Department of Radiology, Turgut Ozal Medical Center, Inonu University School of Medicine, 44069 Malatya, Turkey. E-mail: aalkan@inonu.edu.tr
Received March 4, 2005; Accepted November 30, 2005.
DOI 10.1002/jmri.20518
Published online 2 February 2006 in Wiley InterScience (www.interscience.wiley.com).

Table 1
Magnetic Resonance Imaging Features Related with the Stage in Patients with SSPE

Clinical stage	Cerebral atrophy	Cerebellar atrophy	Brainstem involvement	Periventricular and subcortical hyperintensities	Normal MRI findings
Stage II ($N = 11$)	9% ($N = 1$)	–	9% ($N = 1$)	63.6% ($N = 7$)	36.3% ($N = 4$)
Stage III ($N = 7$)	100% ($N = 7$)	71.4% ($N = 5$)	71.4% ($N = 5$)	100% ($N = 7$)	–
Total ($N = 18$)	44.4 ($N = 8$)	27.7% ($N = 5$)	33.3% ($N = 6$)	77.7% ($N = 14$)	22.2% ($N = 4$)

MATERIALS AND METHODS

A total of 18 patients (14 males and four females) who met the criteria for SSPE disease according to neurological and laboratory findings (i.e., clinical signs and symptoms, characteristic EEG patterns, and high titers of measles antibody in the serum and CSF) were included in our study.

For clinical staging we used the criteria of Jabbour et al (17) (stage I: personality changes and/or behavioral disturbance; stage II: convulsive motor signs, myoclonus, incoordination, choreoathetosis, and tremors; stage III: coma, opistotonus, decerebrate rigidity, and no responsiveness to any stimulus; stage IV: loss of cerebral cortex function, less frequent myoclonus, and diminished hypertonia). The early and late stages represented stages I and II, and stages III and IV, respectively. One clinician experienced in pediatric neurology revealed the examination of each patient. The patients were categorized into two groups: group 1 (stage II) included 11 patients (age range = 44–132 months, mean age = 93.4 ± 28.4 months), and group 2 (stage III) included seven patients (age range = 36–120, mean age = 96 ± 27.7 months). A total of 11 healthy children (age range = 76–144, mean age = 115 ± 37.3 months) constituted the control group. The ethics committee of our institution approved the study protocol, and informed consent was obtained from the parents of juvenile patients and healthy controls. All children with SSPE were sedated with chloral hydrate (dose = 50–70 mg/kg body weight) or midazolam hydrochloride (dose = 0.1 mg/kg) as needed.

The MRI examination consisted of routine imaging and DWI. MRI was performed on a 1.5-T system (Philips, Gyroscan Intera Master, Best, The Netherlands). T1-weighted images (TR = 560 msec, TE = 15 msec) were obtained in the axial and sagittal planes. T2-weighted images (TR = 4530 msec, TE = 100 msec) were obtained in the axial and coronal planes. For DWI a single-shot echo-planar pulse sequence (TR = 4832 msec, TE = 81 msec, field of view (FOV) = 230 mm, matrix size = 128 × 256, slice thickness = 7 mm, interslice gap = 1 mm) was used in all patients and controls with two different b-values (0 and 1000 s/mm^2). We calculated directionally averaged ADCs from the ADC map in circular or elliptical regions of interest (ROIs) drawn on the regions identified on the baseline T2-weighted b = 0 sec/mm^2 images. The ADC maps were reconstructed with commercially available software. In patients and healthy controls, seven distinct neuroanatomic structures (frontal, parieto-occipital, cerebellar, and deep white matter; thalamus; basal ganglia (globus pallidum and putamen); and brainstem (pons)) were selected for analysis in our study because previous studies mentioned that these sites are likely to appear abnormal on MRI (10,15,18).

ADC values were calculated directly from these automatically generated ADC maps with ROI. We minimized partial volume effects by inspecting the slices above and below the region to avoid averaging with CSF. The areas of the ROIs were 120–170 mm^2 in the frontal and parieto-occipital white matter, 110–150 mm^2 in the cerebellar and deep white matter, and 50–120 mm^2 in the basal ganglia, brainstem, and thalamus.

All statistical analyses were performed using a commercially available SPSS release 10.0 software package (SPSS Inc., Chicago, IL, USA). The results are presented as the mean ± standard deviation (SD) to facilitate comprehension of the tables. The distribution of ADC values in patients with SSPE and control groups was abnormal in a one-sample Kolmogorov-Smirnov test. Mann-Whitney's U-test was used to assess whether there is a difference in the ADC values of seven distinct neuroanatomic structures between healthy control group and patients, and between stage II and III patients. A P-value below 0.05 was considered statistically significant.

RESULTS

There was no statistically significant difference in age between patients and controls.

MRI findings related to the stage of patients with SSPE are presented in Table 1. The sensitivity, specificity, and accuracy values were respectively 60%, 87.5%, and 72% in stage II, and 87.5%, 100%, and 94% in stage III patients.

The ADC values obtained from frontal, parieto-occipital, cerebellar, and deep white matter; thalamus; basal ganglia; and brainstem were significantly increased in patients ($N = 18$) compared to control subjects ($P < 0.05$; Table 2).

The ADC values in seven distinct regions were significantly increased in both stage II and III patients compared to the control group ($P < 0.05$).

Table 2
Mean ADC Values of Patients with SSPE

	Mean ADC values ($\times 10^{-6}$mm^2/second)						
	FWM	POWM	CWM	DWM	BG	Thalamus	Brainstem
Stage II ($N = 11$)	1037 ± 175	1015 ± 162	796 ± 107	1081 ± 240	804 ± 47	796 ± 37	819 ± 104
Stage III ($N = 7$)	1350 ± 94	1489 ± 189	1014 ± 182	1518 ± 157	1068 ± 189	1152 ± 352	1018 ± 158
Control ($N = 10$)	786 ± 40	794 ± 30	720 ± 27	756 ± 33	723 ± 43	735 ± 40	740 ± 33

FWM = frontal white matter, POWM = parieto-occipital white matter, CWM = cerebellar white matter, DWM = deep white matter, BG = basal ganglia, ADC = apparent diffusion coefficient.

There were statistically significant differences for ADC values obtained from all locations between the stage II (Fig. 1) and III patients (Fig. 2; $P < 0.05$). The highest mean ADC values were calculated in stage III patients.

DWI disclosed increased diffusion in periventricular and subcortical hyperintensities on T2-weighted images in seven of 11 patients with stage II, and the calculated ADC values were high. Although MRI and DWI findings were normal in the remaining four patients with stage II disease, ADC values were significantly increased compared to controls.

DISCUSSION

SSPE is a rare, progressive neurologic disorder of childhood and early adolescence (15). The diagnosis is based on clinical findings, EEG, and the titer of measles antibodies in the CSF and serum (16). A latent period of 6–8 years follows the primary infection, which usually occurs before the age of 2.

A significant relationship between clinical stage and neuropathological findings was reported in a clinicopathological study (19). Pathologically, mild inflammation of the cortical gray matter is prominent in the earlier period of the disease, which later progresses to subcortical and deep white matter involvement (15). It has been reported that histopathologic examinations show evidence of neuronal loss, astrogliosis, demyelination, and infiltration of inflammatory cells (2,20,21).

Since the clinical profile of the disease involves various presentations, early diagnosis and true clinical staging are not always easy to achieve. The correlation between MRI findings and clinical progression is a controversial issue in the literature (15). Despite the progress of SSPE, improvement of MRI findings may be

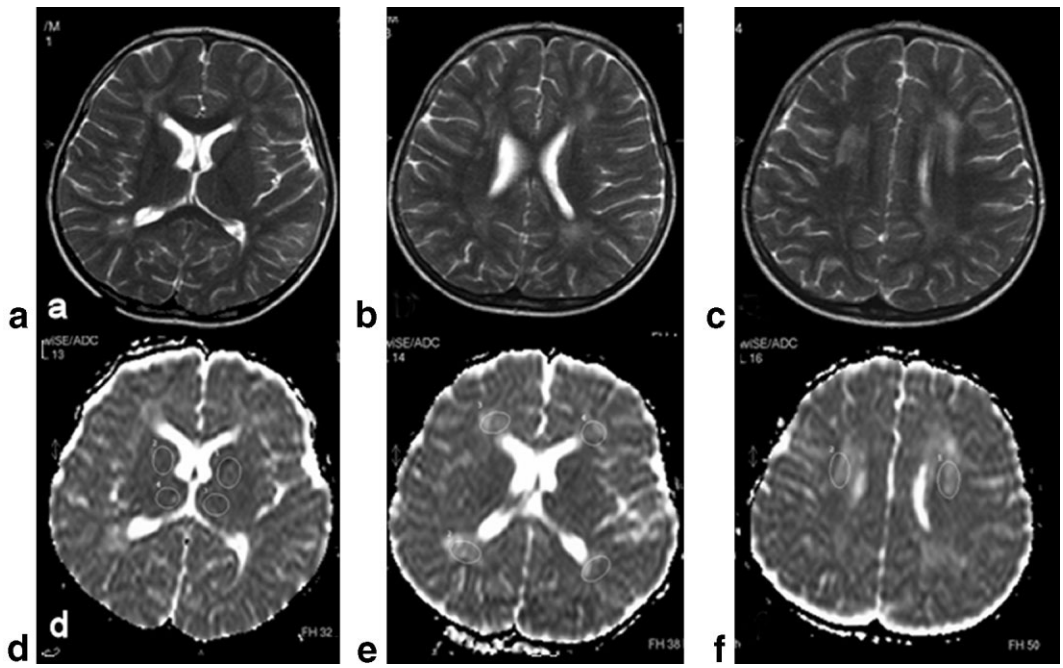

Figure 1. Findings in a 3-year-old girl with stage II SSPE. **a–c:** Axial T2-weighted image (TR = 4530 msec, TE = 100 msec) shows asymmetric high signal intensity lesions in the periventricular white matter. **d:** ADC maps show high ADC values in the basal ganglia (873 and 897 $\times$ 10^{-6}mm^2/sec) and thalamus (846 and 821 $\times$ 10^{-6}mm^2/sec). **e** and **f:** ADC maps reveal high signal intensity and ADC values in the periventricular (1124, 1166, 1197, and 1098 $\times$ 10^{-6}mm^2/sec) and deep white matter (1427 and 1429 $\times$ 10^{-6}mm^2/sec).

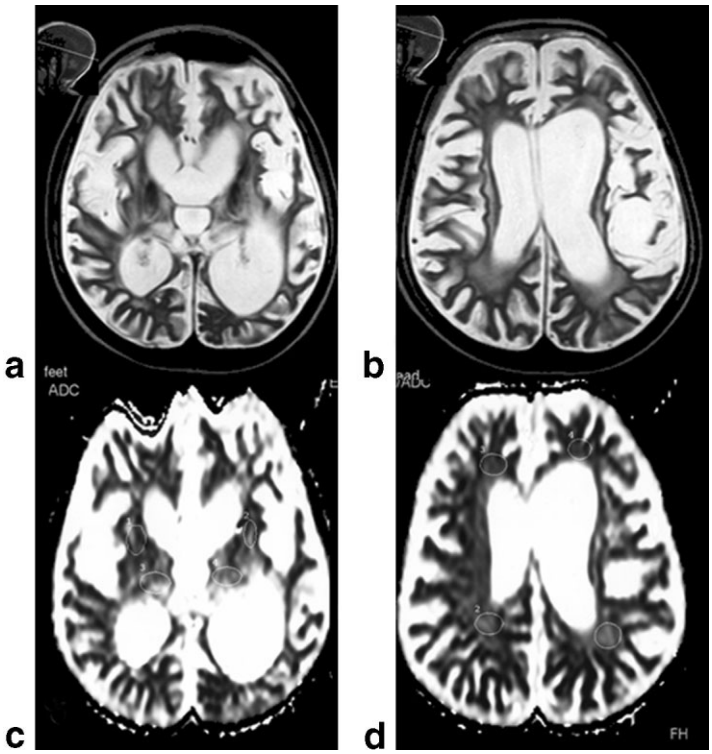

Figure 2. Findings in a 10-year-old boy with stage III SSPE. **a** and **b:** Axial T2-weighted image (TR = 4530 msec, TE = 100 msec) shows hyperintensities in the periventricular white matter, basal ganglia, and thalamus, with marked cerebral atrophy. **c** and **d:** ADC maps reveal high ADC values in the basal ganglia (1352 and 1376 $\times$ $10^{-6}mm^2/sec$), thalamus (1678 and 1631 $\times$ $10^{-6}mm^2/sec$), and periventricular white matter (1613, 1634, 1684, and 1695 $\times$ $10^{-6}mm^2/sec$).

seen. MRI findings may be normal in the early stages (3–7). This discordance could be explained by studies involving neuropathological verification of these lesions (19,22,23).

In our study hyperintensities in the periventricular and subcortical white matters on T2-weighted imaging and ADC maps were detected in 63.6% of stage II patients, and in all stage III patients. MRI and DWI findings were normal in four of 11 patients with stage II disease (36.3%). In one patient with clinical stage II disease, MRI revealed brainstem involvement and cerebral atrophy. The sensitivity, specificity, and accuracy values were respectively 60%, 87.5%, and 72% in stage II, and 87.5%, 100%, and 94% in stage III patients. It is clear that the relationship between MRI findings and the early stages of SSPE was not as strong as that between MRI and late-stage disease in our study.

Although to date SSPE is not completely curable, with early treatment it is possible to slow the progression of disease and improve the patient's quality of life. Since MRI findings do not show an exact correlation with early clinical stages, there is a clear need for new neuroimaging modalities to help recognize the early manifestations of SSPE.

DWI offers investigators an opportunity to evaluate the structural characteristics of tissues (24). It is an important tool for evaluating the random molecular motion of water protons. The ADC reflects the structural properties of the cellular compartments of the tissue studied, and provides a rotationally invariant measurement of the total diffusion of water within a tissue (12,24,25). DWI is useful for diagnosing diseases with cytotoxic edema, since it can be used to differentiate cytotoxic from vasogenic edema. In cytotoxic edema the reduced ADC, which appears as hyperintensity on DWI, is related to increased intracellular space and decreased extracellular space as water shifts from extracellular to intracellular space. In vasogenic edema the ADC is normal or increased, which presumably depends on increased extracellular space as water shifts from the blood vessel (26).

In demyelinating disease the myelin structure and neuronal loss lead to an expansion of the extracellular space, which results in an increased ADC (10,11,25). It has also been reported that the progressive increase in ADC values in patients with demyelinating disease correlates with the cessation of inflammatory activity and the progression of tissue damage (25).

In the literature, DWI findings of SSPE have been reported as elevated diffusion rates, which may reflect some disintegration of the tissue in the lesions of SSPE (10,11). The higher ADC values in these parenchymal lesions suggest that there is a relatively high molecular motion in these regions compared to normal brain parenchyma. This probably represents so-called demyelination and neuronal loss, a well known histopathologic feature of SSPE (2,10,11,20,21).

Lee et al (18) and Sener (9) reported different DWI patterns in studies related to acute encephalitis due to measles infection. The DWI patterns of lesions were consistent with those of cytotoxic edema associated with acute infection. In our study, high ADC values consistent with vasogenic edema were calculated in seven distinct locations in patients. There were differences in ADC values between stage II and III patients (Fig. 3). The highest mean ADC values were calculated in stage III patients. When clinical stages

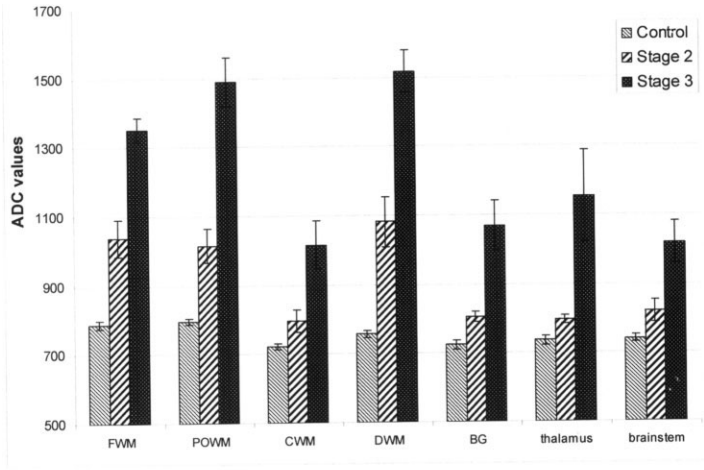

Figure 3. Mean ADC values ($\times 10^{-6}$mm^2/sec) obtained from frontal, parieto-occipital, cerebellar, and deep white matter; thalamus; basal ganglia; and brainstem are higher in stage III patients with SSPE compared to stage II patients and healthy control subjects.

FWM: Frontal white matter
POWM: Parieto-occipital white matter
CWM: Cerebellar white matter
DWM: Deep white matter
BG: Basal ganglia
ADC: Apparent diffusion coefficient (x10^{-6}mm^2/s)

were compared with abnormal ADC values, the white matter in particular revealed more prominent ADC values (Table 2). These findings may represent demyelination and neuronal loss (10,11). DWI disclosed increased diffusion in the periventricular and subcortical hyperintensities on T2-weighted images in seven of 11 patients with stage II, and the calculated ADC values were high. Although the remaining four patients had normal MRI and DWI findings, calculated ADC values from normal-appearing regions were increased compared to controls (Fig. 4). Oksuzler et al (11) also reported high ADC values in NAWM regions on DWI in a patient with SSPE. The increased ADC values obtained from normal-appearing regions in patients with SSPE in the present study may support the notion of histopathologic changes, as proposed in a previous study (11). Our results indicate a progressive increase in ADC values in accordance with the clinical stage that may depend on advancing neuronal loss and demyelination development.

In conclusion, the increased ADC values observed in our study suggest increased mobility of water molecules in the brain parenchyma of patients with SSPE. This vasogenic edema-like pattern probably corresponds to necrosis, inflammation, demyelination, neuronal loss, and gliosis, which are among the reported histopathological changes induced by SSPE (10,11). The stage of disorder may be independent of

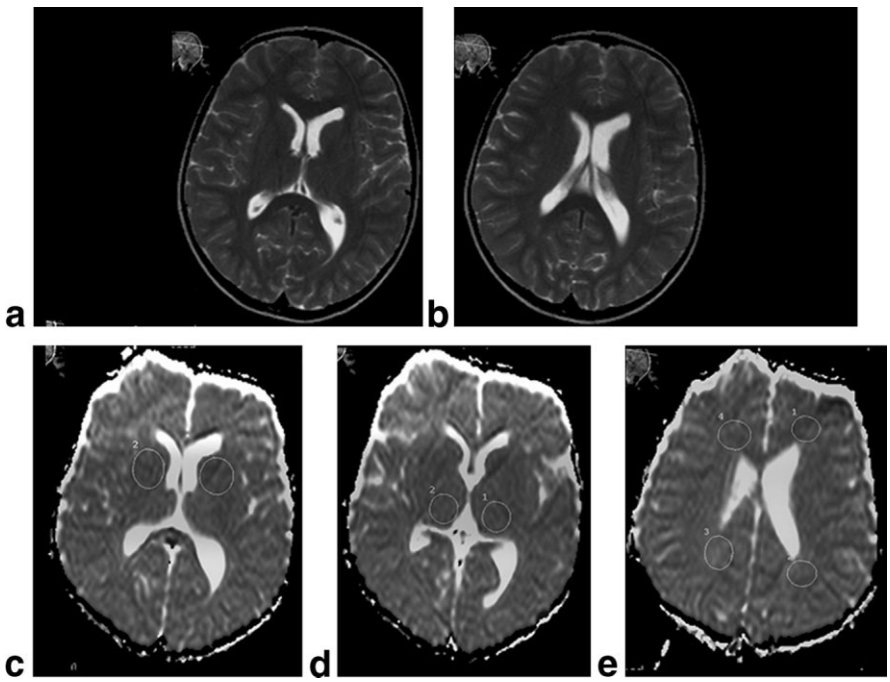

Figure 4. Findings in a 9-year-old girl with stage II SSPE. **a** and **b:** Axial T2-weighted image (TR = 4530 msec, TE = 100 msec) shows normal signal intensity in the periventricular white matter, basal ganglia, and thalamus. **c–e:** ADC maps reveal high ADC values in the basal ganglia (873 and 877 $\times$ 10^{-6}mm^2/sec), thalamus (838 and 841 $\times$ 10^{-6}mm^2/sec), and periventricular white matter (871, 900, 912, and 924 $\times$ 10^{-6}mm^2/sec, respectively).

DWI appearance, even though the brain is affected. Therefore, DWI and ADC values supplemental to routine MRI should also be utilized for lesion detection and definition, which will enhance diagnostic accuracy for patients with SSPE.

REFERENCES

1. Graves MC. Subacute sclerosing panencephalitis. Symposium on neurovirology. Neurol Clin 1984;2:267–280.
2. Garg RK. Subacute sclerosing panencephalitis. Postgrad Med J 2002;78:63–70.
3. Ozturk A, Gurses C, Baykan B, Gokyiğit A, Eraksoy M. Subacute sclerosing panencephalitis: clinical and magnetic resonance imaging evaluation of 36 patients. J Child Neurol 2002;17:25–29.
4. PeBenito R, Naqvi SH, Arca MM, Schubert R. Fulminating subacute sclerosing panencephalitis: case report and literature review. Clin Pediatr 1997;36:149–154.
5. Yaqup BA. Subacute sclerosing panencephalitis (SSPE): early diagnosis, prognostic factors and natural history. J Neurol Sci 1996; 139:227–234.
6. Dietrich RB, Vining EP, Taira RK, Hall TR, Phillipart M. Myelin disorders of childhood: correlation of MR findings and severity of neurological impairment. J Comput Assist Tomogr 1990;14:693–698.
7. Winer JB, Pires M, Kermode A, Ginsberg L, Rossor M. Resolving MRI abnormalities with progression of subacute sclerosing panencephalitis. Neuroradiology 1991;33:178–180.
8. Alkan A, Sarac K, Kutlu R, et al. Early and late state subacute sclerosing panencephalitis: chemical shift imaging and single-voxel MR spectroscopy. AJNR Am J Neuroradiol 2003;24:501–506.
9. Sener RN. Subacute sclerosing panencephalitis with pontine involvement. J Comput Assist Tomogr 2004;28:101–102.
10. Sener RN. Subacute sclerosing panencephalitis findings at MR imaging, diffusion MR imaging and proton MR spectroscopy. AJNR Am J Neuroradiol 2004;25:892–894.
11. Oksuzler YF, Cakmakci H, Kurul S, Oksuzler M, Dirik E. Diagnostic value of diffusion-weighted magnetic resonance imaging in pediatric cerebral diseases. Pediatr Neurol 2005;32:325–333.
12. Caramia F, Pantano P, Di Legge S, et al. A longitudinal study of MR diffusion changes in normal appearing white matter of patients with early multiple sclerosis. Magn Reson Imaging 2002;20:383–388.
13. Schaefer PW. Applications of DWI in clinical neurology. J Neurol Sci 2001;186:25–35.
14. Provenzale JM, Sorensen AG. Diffusion-weighted MR imaging in acute stroke: theoretic considerations and clinical applications. AJR Am J Roentgenol 1999;173:1459–1467.
15. Tuncay R, Akman-Demir G, Gokyigit A, et al. MRI in subacute sclerosing panencephalitis. Neuroradiology 1996;38:636–640.
16. Anlar B, Saatci I, Kose G, Yalaz K. MRI findings in subacute sclerosing panencephalitis. Neurology 1996;47:1278–1283.
17. Jabbour JT, Garcia JH, Lemmi H, Ragland J, Duenas DA, Sever JL. Subacute sclerosing panencephalitis presenting as simple partial seizures. J Child Neurol 1990;5:146–149.
18. Lee KY, Cho WH, Kim SH, Kim HD, Kim IO. Acute encephalitis associated with measles: MRI features. Neuroradiology 2003;45: 100–106.
19. Begeer JH, Haaxma R, Snoek JW, Boonstra S, le Coultre R. Signs of focal posterior cerebral abnormality in early subacute sclerosing panencephalitis. Ann Neurol 1986;90:200–202.
20. Dyken PR. Subacute sclerosing panencephalitis: current status. Neurol Clin 1985;3:179–196.
21. Tsuchiya K, Yamauchi T, Furui S, Suda Y, Takenaka E. MR imaging vs CT in subacute sclerosing panencephalitis. AJNR Am J Neuroradiol 1988;9:943–946.
22. Ohya T, Martinez AJ, Jabbour JT, Lemmi H, Duenas DA. Subacute sclerosing panencephalitis: correlation of clinical, neurophysiologic, and neuropathologic findings. Neurology 1974;24:211–218.
23. Brismar J, Gascon GG, von Steyern KV, Bohlega S. Subacute sclerosing panencephalitis: evaluation with CT and MR. AJNR Am J Neuroradiol 1996;17:761–772.
24. Roychowdhury S, Maldjian JA, Grossman RI. Multiple sclerosis: comparison of trace apparent diffusion coefficients with MR enhancement pattern of lesions. AJNR Am J Neuroradiol 2000;21: 869–874.
25. Rovira A, Pericot I, Alonso J, Rio J, Grive E, Montalban X. Serial diffusion-weighted MR imaging and proton MR spectroscopy of acute large demyelinating brain lesions: case report. AJNR Am J Neuroradiol 2002;23:989–994.
26. Moritani T, Shrier DA, Numaguchi Y, et al. Diffusion-weighted echo-planar MR imaging: clinical applications and pitfalls—a pictorial essay. Clin Imaging 2000;24:181–192.